Biochemical and Biophysical Research Communications 404 (2011) 297–301

Contents lists available at ScienceDirect

Biochemical and Biophysical Research Communications

journal homepage: www.elsevier.com/locate/ybbrc

Determining the binding mode and binding affinity constant of tyrosine kinase inhibitor PD153035 to DNA using optical tweezers

Chih-Ming Cheng [a,c,e], Yuarn-Jang Lee [d,1], Wei-Ting Wang [a,b,c], Chien-Ting Hsu [b,c], Jing-Shin Tsai [a,b,c], Chien-Ming Wu [e], Keng-Liang Ou [b,c], Tzu-Sen Yang [a,b,c,*]

[a] School of Dental Technology, Taipei Medical University, Taipei 110, Taiwan
[b] Institute of Biomedical Materials and Engineering, Taipei Medical University, Taipei 110, Taiwan
[c] Research Center for Biomedical Implants and Microsurgery Devices, Taipei Medical University, Taipei 110, Taiwan
[d] Section of Infectious Diseases, Department of Internal Medicine, Taipei Medical University Hospital, Taipei 110, Taiwan
[e] Department of Biomedical Engineering and Environmental Sciences, National Tsing Hua University, Hsinchu 30043, Taiwan

ARTICLE INFO

Article history:
Received 20 October 2010
Available online 2 December 2010

Keywords:
PD153035
Non-small cell lung cancer
Tyrosine kinase inhibitor
Binding affinity constant
Optical tweezers
Wormlike chain model

ABSTRACT

Accurately predicting binding affinity constant (K_A) is highly required to determine the binding energetics of the driving forces in drug–DNA interactions. Recently, PD153035, brominated anilinoquinazoline, has been reported to be not only a highly selective inhibitor of epidermal growth factor receptor but also a DNA intercalator. Here, we use a dual-trap optical tweezers to determining K_A for PD153035, where K_A is determined from the changes in B-form contour length (L) of PD153035–DNA complex. Here, L is fitted using a modified wormlike chain model. We found that a noticeable increment in L in 1 mM sodium cacodylate was exhibited. Furthermore, our results showed that $K_A = 1.18(\pm 0.09) \times 10^4$ (1/M) at 23 ± 0.5 °C and the minimum distance between adjacent bound PD153035 ≈ 11 bp. We anticipate that by using this approach we can determine the complete thermodynamic profiles due to the presence of DNA intercalators.

1. Introduction

Lung cancer is the leading cause of cancer-related death worldwide. Primary lung cancers include small cell lung cancer (SCLC) and non-small cell lung cancer (NSCLC), and the occurrence of NSCLC accounts for most cases (about 85% of all lung cancers) [1]. The primary treatment for NSCLC usually involves chemotherapy and targeted therapy. Cisplatin is one of the chemotherapy drugs used to treat advanced NSCLC because it attaches to DNA and disrupts repair. Concerning the targeted therapy, because epidermal growth factor receptor (EGFR) is highly expressed (88–99%) in NSCLC [2–4], EGFR tyrosine kinase inhibitors have become particularly promising targeted drugs for treating NSCLC. In the past, quinazolones, such as PD153035 (Fig. 1), have been identified as a new class of tyrosine kinase inhibitors [5]. On the other hand, recent studies also reveal that PD153035 directly intercalates into the DNA [6–8], which suggests that PD153035, the multitargeting drug, bears great potential for human cancer treatment [7]. However, the binding affinity constant (K_A) and the change of binding free energy (ΔG) for PD153035 cannot be determined using bulk fluorescence titration experiments due to that changes in fluorescence emission are very weak [6]. Hence, the objective of this study is to address this pharmacological issue.

Single-molecule methods, such as the use of atomic force microscopy (AFM) [9], magnetic tweezers [10], and optical tweezers [11–18], have been employed to probe both the molecular interactions and the mechanical properties of individual ligand–DNA complexes. Additionally, scanning force microscopy (SFM) [19] and optical tweezers [11–14] have been employed to further investigate K_A and site exclusion number (n)—the minimum distance in base pairs between adjacent bound intercalator molecules—of an intercalating agent. The SFM method measures the contour length of DNA molecules in the absence of a stretching force to estimate both K_A and n [19]. However, both K_A and n could be determined through single-molecule DNA stretching using optical tweezers, which can measure changes in either the DNA molecular length [11,12,14] or contour length [13] in various intercalator concentrations. In past work [13], we presented an alternative wormlike chain (WLC) model-based approach to directly determine the zero-force binding energetics of an intercalated DNA complex by measuring the zero-force B-form DNA contour length, which is determined by the WLC model. To implement successive stretch–relax cycles for single DNA molecules, we have constructed

* Corresponding author at: School of Dental Technology, Taipei Medical University, 250 Wu-Hsing Street, Taipei 110, Taiwan.
E-mail address: tsyang@tmu.edu.tw (T.-S. Yang).
[1] Co-first author.

0006-291X/$ - see front matter © 2010 Elsevier Inc. All rights reserved.
doi:10.1016/j.bbrc.2010.11.110

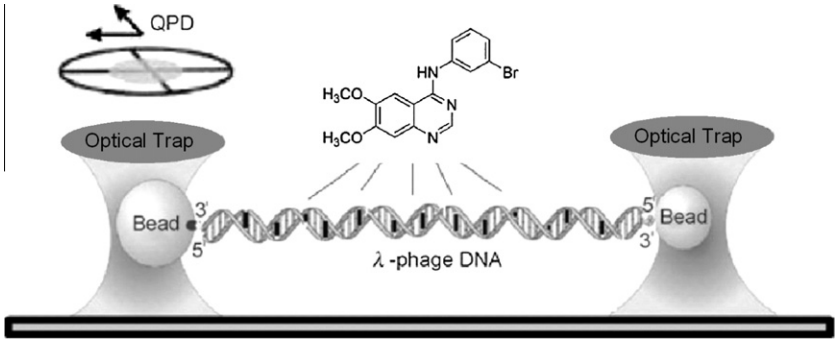

Fig. 1. Schematic representation of the single-molecule approach to study drug–DNA interaction. The figure presents the experimental setup used to implement successive stretch–relax cycles for the bacteriophage λ-DNA in various concentrations of intercalating agent PD153035. The PD153035 can be inserted between Watson–Crick base pairs. The high-resolution optical tweezers system comprises two independently controlled optical traps, in which one trapping laser is controlled using a scan mirror as the fixed trap (left-hand side) and the other is controlled using another scan mirror as the scanning trap (right-hand side). The QPD, in the upper left, is the position sensor, which is used to determine the corresponding tension on the DNA molecule.

a dual-trap optical tweezers instrument (Fig. S1 of Supplementary material). We will apply this single-molecule approach that allows direct investigating the effect of ionic strength on the binding mode of PD153035 to DNA, the DNA mechanical properties in the absence and presence of PD153035, and determining both K_A and n for PD153035 for the first time.

2. Methods

2.1. Experimental system

The optical tweezers system (Fig. S1 of Supplementary material) is integrated into a commercial inverted optical microscope (TE2000U, Nikon) and incorporates two lasers for trapping and position detection. This system is similar to the one developed by Block and colleagues [20]. A two-trap optical tweezers system is applied to conduct a single-DNA-molecule stretching experiment; one trapping laser is controlled using a antireflection mirror as the fixed trap and the other is controlled using a scanning mirror (6240H, Cambridge Technology) as the scanning trap. For position detection, a quadrant photodiode (QPD, model SPOT-9D, UDT) is used to capture a position signal for the bead location, where the position signal can be measured with bandwidths up to 100 kHz larger than the characteristic frequency due to Brownian motion. In terms of the position detection scheme, we apply the far-field interference method [21], where the interference of an outgoing detection laser light with scattered light from the trapped particle occurs at the condenser's back focal plane, and the corresponding interference pattern is imaged onto a QPD. Here, we use a Nd:YAG laser (1064 nm, VA-II-N-1064) as a trapping laser. However, a separate laser (830 nm, GLM-L3IF-100) is selected as a detection laser.

2.2. Molecular construction of dumbbell DNA

To construct the DNA–bead complex, the biotinylated ends of the bacteriophage λ-DNA (48,502 bp, New England Biolabs) fragment, which were ligated by T4 DNA ligase (New England Biolabs), were attached to streptavidin-coated beads of 1.87 μm mean diameter (Spherotech) in a TE buffer (pH 8.0) that contained sodium cacodylate at millimolar concentrations.

2.3. Molecular interaction of the PD153035 with DNA

Recent studies have shown that PD153035 is insoluble in water but can be dissolved in dimethyl sulfoxide (DMSO). However, the density of DMSO is larger than that of the streptavidin-coated polystyrene beads. Therefore, minimizing the buoyancy effect on the trapped beads is necessary to facilitate single-molecule manipulation with a 1.4 numerical aperture objective. To this end, Tween 80 was used to enhance the solubility of PD153035; therefore, PD153035 (Merck) dissolved in DMSO was further diluted with Tween 80 to avoid aggregation (Fig. S2 of Supplementary material). Then, the DNA–bead complex was incubated with the PD153035 at different concentration ranging from 0 to 200 μM. After both of these beads had been connected in the form of a dumbbell, each was held in a separate optical trap, so that single-DNA-molecule stretching experiments could be conducted (Fig. 1). During the experiments, the concentrations of sodium cacodylate, DMSO, and Tween 80 were 1 mM, 1%, and 4%, respectively; bacteriophage λ-DNA concentration was 0.17 pM, which was determined using a Qubit (Invitrogen) fluorometer. On the other hand, previous studies have shown that, at higher ionic strength (16 mM Na^+), the binding of PD153035 to DNA is reduced [6]. For this reason, we will investigate the effect of ionic strength (from 1 to 50 mM for monovalent salt) on the binding of PD153035 to DNA in more detail.

3. Results and discussion

3.1. Single-molecule stretching experiments

To quantify the DNA elastic properties, the stretching behavior of DNA can be fitted properly using the modified Marko–Siggia WLC model that takes into account the stretching of the DNA at or slightly beyond full extension [15–18,22]:

$$F = \left(\frac{k_B T}{L_P}\right)\left\{\left[\frac{1}{4(1 - x/L + F/S)^2}\right] - \frac{1}{4} + \frac{x}{L} - \frac{F}{S}\right\}. \quad (1)$$

Here, F is the tension on the DNA molecule, L_p is the persistence length of the DNA molecule, T is the temperature, x is the DNA molecular length, L is the zero-force B-form contour length; k_B is the Boltzmann constant, and S is the elastic stretch modulus. Therefore, the zero-force B-form contour length of the DNA molecule in the absence and presence of PD153035, together with values of the persistence length and the elastic stretch modulus, can be extracted by fitting the F–x curve to Eq. (1) using the Ezyfit, a free-curve-fitting toolbox for Matlab (The MathWorks).

In an attempt to obtain equilibrium binding energetic information, including equilibrium binding affinity constant, and change of binding free energy through DNA stretching with a two-trap optical tweezers system, at first we had to verify whether the mechanical stretching process in the presence of various concentrations of PD153035 is in equilibrium. For a DNA molecule in the presence of

75 μM PD153035, both stretch and relax cycles are associated with almost coincidental *F–x* curves, where the stretching velocity and a sampling rate are 0.5 μm/s and 50 Hz, respectively (Fig. S3 of Supplementary material). This finding indicates that hysteresis does not occur under this stretching velocity, namely, the PD153035–DNA complex is in equilibrium in the applied force regime of $F < 40$ pN. By fitting the *F–x* curve using Ezyfit, the DNA B-form contour length is about 17.08 μm in the presence of 75 μM PD153035.

3.2. Effect of monovalent ionic strength on PD153035 binding to DNA

Nowadays two characteristics are applied to identify whether the mode-of-binding to DNA is an intercalator, including either the existence of a well-defined isosbestic point in the absorption spectra or the simultaneously lengthening the helix due to the presence of DNA-binding drugs. In the case of PD153035, as mentioned earlier, changes in fluorescence emission are very weak; for this reason, we apply single-molecule stretching experiments to evaluate the binding mode of PD153035 to DNA and effect of monovalent ionic strength on the elasticity of single native DNA molecules in the absence and presence PD153035.

The B-form contour lengths of the native DNA molecule at different monovalent ionic strengths were extracted by fitting the *F–x* curve using the Ezyfit; these are listed in Table S1 of Supplementary material. Similarly, we further tested the effect of monovalent ionic strength on the B-form DNA contour lengths in the presence of PD153035; the B-form contour lengths of the PD153035–DNA complex are listed in Table S2 of Supplementary material. The values of B-form contour length for native DNA did not differ significantly from those observed in monovalent salt. However, as for the PD153035–DNA complex, ionic strength had a significant influence on the contour length. At a higher ionic strength (e.g., 35 mM NaCl, 35 mM sodium cacodylate), PD153035 may have weak DNA-binding ability for DNA in the presence of 100 μM PD153035. In contrast to that in the higher ionic strength condition, a noticeable increment in the B-form contour length at very low salt concentration (e.g., 1 mM sodium cacodylate) was exhibited, which suggests that the mode-of-binding to DNA is an intercalator. A possible explanation for an increment in the B-form contour lengths of individual PD153035–DNA complex is that there exists localized melting in AT-rich regions and intramolecular electrostatic repulsion at low salt concentration [18], namely, DNA becomes more susceptible to enthalpic elongation. This mechanism may promote PD153035 intercalation. However, low salt conditions are also some of the worst conditions for studying intercalation by stretching a single DNA molecule. During these experiments, for instance, the average ratios of a successful assembly of λ-DNA molecule tethered between two streptavidin-coated beads were 10:5:1, when ionic strengths were 50 mM, 35 mM, and 1 mM, respectively. This observation indicated that there exists a strong ionic strength influence on the stability of B-form DNA structure.

3.3. Binding affinity constant and site exclusion number analyses

By conducting DNA stretching measurements, we can obtain *F–x* curves at different PD153035 concentrations ranging from 0 to 200 μM. The measured *F–x* curves are fit to the modified Marko–Siggia WLC model in the absence and presence of PD153035 (Fig. S4 of Supplementary material), where the *F–x* curves and the corresponding WLC model fittings of λ-DNA in the absence (circle symbol) and presence of PD153035 concentrations of 75 μM (diamond symbol) and 100 μM (square symbol) are shown

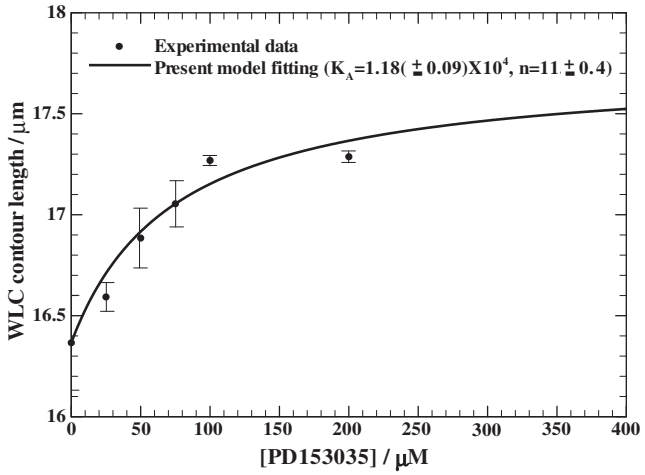

Fig. 3. The *F–x* curves of single λ-DNA molecule coexisting with PD153035 in various concentrations from 0 to 200 μM. Here, only *F–x* curves of PD153035 concentrations of 0 (circle symbol), 75 (diamond symbol), and 100 μM (square symbol) are shown for simplicity. In these experiments, the stretching velocity and the sampling rates are 0.5 μm/s and 50 Hz, respectively.

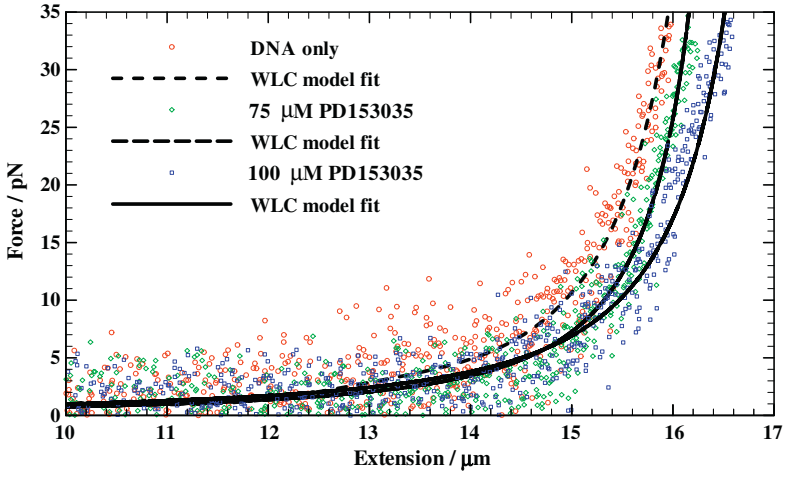

Fig. 2. Mechanical responses of single λ-DNA molecule mixed with PD153035, where the concentrations of λ-DNA, sodium cacodylate, DMSO, and Tween 80 were 0.17 pM, 1 mM, 1%, and 4%, respectively. For the DNA molecule in the presence of 75 μM PD153035, both stretch and relax cycles are associated with almost coincidental *F–x* curves.

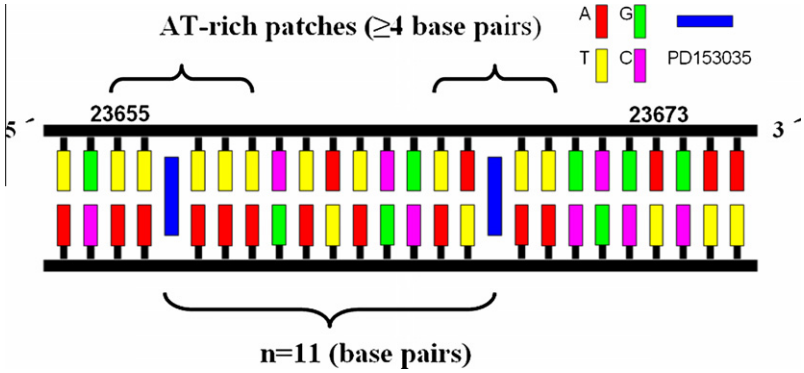

Fig. 4. Schematic picture of the PD153035 molecule intercalated in λ-DNA molecule. This scenario showed two possible PD153035 intercalating sites within the nucleotide sequence of λ-DNA fragment at 23,653–23,676 kbp, where the minimum distance between adjacent bound PD153035 ≈ 11 bp and PD153035 tended to intercalate at AT-rich sequences covering at least 4 bp.

in Fig. 2 for simplicity. We found that there existed mechanical responses of single λ-DNA molecule coexisted with PD153035, in which the binding of PD153035 to λ-DNA began to saturate at about 100 μM. The binding of PD153035 indeed lengthened the DNA molecule at very low salt concentration and was accompanied by a shift in the *F–x* curves to larger extension values.

As noted earlier, values of the persistence length L_p and the elastic stretch modulus S can also be determined using Eq. (1). The results showed that there existed a dependence of L_p and S on PD153035 concentrations (Figs. S5 and S6 of Supplementary material). Points and error bars are mean and standard deviations of L_p and S, respectively. As can be seen, the L_p is about 110 nm in the absence of PD153035 and value of L_p at higher PD153035 concentration is near 42 nm. On the other hand, S was about 900 pN in the absence of PD153035 and the value of S at higher PD153035 concentration was near 750 pN. The results indicated that both L_p and S were reduced by the presence of the intercalating agent, which suggests that the DNA molecules became softer due to the presence of PD153035.

In our previous studies [13], we have attempted to follow the same expression [19] to estimate the K_A of intercalating agent under zero-force condition. Since the fractional increase in DNA contour length is directly related to the fraction of occupied intercalation sites at a given intercalator concentration, K_A is therefore explicitly related to the measured DNA contour length by

$$K_A = \frac{\left(\frac{L-L_0}{a}\right)[DNA]}{\left(\left(\frac{[DNA]B}{n}\right) - \left(\frac{L-L_0}{a}\right)[DNA]\right)\left(I_D - \left(\frac{L-L_0}{a}\right)[DNA]\right)}, \quad (2)$$

where L_0 and L are the zero-force B-form contour lengths of the DNA molecule in the absence and presence of an intercalated ligand, respectively; a is the lengthening per intercalation, I_D is the total intercalator concentration, [*DNA*] is the total DNA concentration, and B is number of base pairs per DNA molecule. In this study, both L_0 and L were determined by fitting the *F–x* curve using Ezyfit from the entire force regime. Under zero-force condition, the lengthening per intercalation, a, which is attributed to intercalation by the planar aromatic molecule, equals 0.34 nm [23] as adopted in this study.

Fig. 3 depicts the zero-force lengthening data—i.e., the zero-force B-form contour length corresponding to each PD153035 concentration. Each data point is based on at least five experimental stretching measurements, and the corresponding error bars represent the standard deviations of the zero-force B-form contour lengths. The zero-force lengthening data were further fitted using Eq. (2) by the least-square method to yield $K_A = 1.18(\pm 0.09) \times 10^4$ (1/M) (in which the error bar represents 95% confidence interval) and the site exclusion number $n = 11 \pm 0.4$ (Fig. 3). Note that the minimum distance between adjacent bound PD153035 ≈ 11 bp, which indicates that the number of PD153035 molecules occupy an average of 4409 of the intercalation sites on single λ-DNA molecule. Because the complete nucleotide sequence of λ-DNA has been reported [24], we can calculate and determine the numbers of the AT-rich patches as a function of length of the AT-rich patches for λ-DNA molecule (Fig. S7 of Supplementary material). If there exists localized melting in AT-rich regions at low salt concentration [18], we speculate that the minimum length of the AT-rich patches is 4 bp such that both the numbers of the AT-rich patches and the occupied intercalation sites are almost the same (Fig. S7 of Supplementary material). Here, we construct a simple model to demonstrate the scenario when the DNA molecule becomes saturated with PD153035. Fig. 4, for example, schematically showed two possible PD153035 intercalating sites within the nucleotide sequence of λ-DNA fragment at 23,653–23,676 bp; this scenario follows the aforementioned conditions, that is, the minimum distance between adjacent bound PD153035 ≈ 11 bp and PD153035 tended to intercalate at AT-rich sequences covering at least 4 bp. On the other hand, based on van't Hoff equation [25], $\Delta G_{obs} = -RT\ln(K_A)$, the change of binding free energy of PD153035–DNA interaction is -5.49 kcal mol^{-1} calculated at 23 ± 0.5 °C, where a negative change in free energy indicated that the PD153035 interaction tends to occur spontaneously.

4. Conclusions

In the present work, we adopted a WLC model-based approach to determine the binding mode and zero-force binding affinity constant of tyrosine kinase inhibitor PD153035 to DNA by stretching a single DNA molecule. The proposed single-molecule approach provided clear evidence that there is an increment in B-form contour length at very low salt concentration, which suggests that the mode-of-binding to DNA is an intercalator. In addition, we have extended this single-molecule approach to determine both K_A and n of PD153035 for the first time. However, this study showed that PD153035, although this drug exhibits a noticeable increment in the B-form contour lengths of individual PD153035–DNA complex at 1 mM sodium cacodylate, have weak DNA-binding ability at physiological salt concentrations (100 mM for monovalent salt), which implied that inside the nucleus, changes in the chromatin structure contribute to the RAR-β-inducing effect of PD153035 [8] may not occur. We are currently applying the proposed approach, together with our home-made temperature control system to construct complete thermodynamic profiles for the intercalative

drug binding to DNA and these results will be reported in the near future.

Acknowledgments

C.M. Cheng and W.T. Wang contributed equally to this work. We acknowledge funding from the Taipei Medical University (TMU96-AE1-B36), Cathay General Hospital/Taipei Medical University (97CGH-TMU-15), and Taipei Medical University/Taipei Medical University Hospital (98TMU-TMUH-03-3 and 99TMU-TMUH-03-4).

Appendix A. Supplementary data

Supplementary data associated with this article can be found, in the online version, at doi:10.1016/j.bbrc.2010.11.110.

References

[1] R.S. Herbst, J.V. Heymach, S.M. Lippman, Lung cancer, N. Engl. J. Med. 359 (13) (2008) 1367–1380.
[2] V. Rusch, J. Baselga, C. Cordon-Cardo, J. Orazem, M. Zaman, S. Hoda, J. McIntosh, J. Kurie, E. Dmitrovsky, Differential expression of the epidermal growth factor receptor and its ligands in primary non-small cell lung cancers and adjacent benign lung, Cancer Res. 53 (1993) 2379–2385.
[3] G. Fontanini, M. De Laurentiis, S. Vignati, S. Chine, M. Lucchi, V. Silvestri, A. Mussi, S. De Placido, G. Tortora, A.R. Bianco, W. Gullick, C.A. Angeletti, G. Bevilacqua, F. Ciardiello, Evaluation of epidermal growth factor-related growth factors, receptors, of neoangiogenesis in completely resected stage i–iiia non-small-cell lung cancer: amphiregulin and microvessel count are independent prognostic indicators of survival, Clin. Cancer Res. 4 (1998) 241–249.
[4] Y.R. Chen, Y.N. Fu, C.H. Lin, S.T. Yang, S.F. Hu, Y.T. Chen, S.F. Tsai, S.F. Huang, Distinctive activation patterns in constitutively active and gefitinib-sensitive EGFR mutants, Oncogene 25 (8) (2006) 1205–1215.
[5] D.W. Fry, A.J. Kraker, A. McMichael, L.A. Ambroso, J.M. Nelson, W.R. Leopold, R.W. Connors, A.J. Bridges, A specific inhibitor of the epidermal growth factor receptor tyrosine kinase, Science 265 (1994) 1093–1095.
[6] J.F. Goossens, E. Bouey-Bencteux, R. Houssin, J.P. Hénichart, P. Colson, C. Houssier, W. Laine, B. Baldeyrou, C. Bailly, DNA interaction of the tyrosine protein kinase inhibitor PD153035 and its N-methyl analogue, Biochemistry 40 (2001) 4663–4671.
[7] T.W. Grunt, K. Tomek, R. Wagner, K. Puckmair, B. Kainz, D. Rünzler, A. Gaiger, G. Köhler, C.C. Zielinski, Upregulation of retinoic acid receptor-beta by the epidermal growth factor-receptor inhibitor PD153035 is not mediated by blockade of ErbB pathways, J. Cell. Physiol. 211 (2007) 803–815.
[8] T.W. Grunt, K. Tomek, R. Wagner, K. Puckmair, C.C. Zielinski, The DNA-binding epidermal growth factor-receptor inhibitor PD153035 and other DNA-intercalating cytotoxic drugs reactivate the expression of the retinoic acid receptor-beta tumor-suppressor gene in breast cancer cells, Differentiation 75 (9) (2007) 883–890.
[9] R. Krautbauer, H. Clausen-Schaumann, H.E. Gaub, Cisplatin changes the mechanics of single DNA-molecules, Angew. Chem. 112 (2000) 4056–4059.
[10] J. Lipfert, S. Klijnhout, N.H. Dekker, Torsional sensing of small-molecule binding using magnetic tweezers, Nucleic Acids Res. 38 (20) (2010) 7122–7132.
[11] M.J. McCauley, M.C. Williams, Mechanisms of DNA binding determined in optical tweezers experiments, Biopolymers 85 (2007) 154–168.
[12] I.D. Vladescu, M.J. McCauley, M.E. Nunez, I. Rouzina, M.C. Williams, Quantifying force-dependent and zero-force DNA intercalation by single-molecule stretching, Nat. Methods 4 (2007) 517–522.
[13] T.S. Yang, Y. Cui, C.M. Wu, J.M. Lo, C.S. Chiang, W.Y. Shu, W.J. Chung, C.S. Yu, K.N. Chiang, I.C. Hsu, Determining the zero-force binding energetics of an intercalated DNA complex by a single-molecule approach, Chemphyschem 10 (2009) 2791–2794.
[14] C. leimann, A. Sischka, A. Spiering, L. Tönsing, N. Sewald, U. Diederichsen, D. Anselmetti, Binding kinetics of bisintercalator Triostin A with optical tweezers force mechanistics, Biophys. J. 97 (2009) 2780–2784.
[15] M.D. Wang, H. Yin, R. Landick, J. Gelles, S.M. Block, Stretching DNA with optical tweezers, Biophys. J. 72 (1997) 1335–1346.
[16] C.G. Baumann, V.A. Bloomfield, S.B. Smith, C. Bustamante, M.D. Wang, S.M. Block, Stretching of single collapsed DNA molecules, Biophys. J. 78 (2000) 1965–1978.
[17] I. Tessmer, C.G. Baumann, G.M. Skinner, J.E. Molloy, J.G. Hoggett, S.J.B. Tendler, S. Allen, Mode of drug binding to DNA determined by optical tweezers force spectroscopy, J. Mod. Opt. 50 (2003) 1627–1636.
[18] C.G. Baumann, S.B. Smith, V.A. Bloomfield, C. Bustamante, Ionic effects on the elasticity of single DNA molecules, Proc. Natl. Acad. Sci. USA 94 (1997) 6185–6190.
[19] J.E. Coury, L. McFail-Isom, L.D. Williams, L.A. Bottomley, A novel assay for drug–DNA binding mode, affinity, and exclusion number: scanning force microscopy, Proc. Natl. Acad. Sci. USA 93 (1996) 12283–12286.
[20] J.M. Lang, C.L. Asbury, J.W. Shaevits, S.M. Block, An automated two-dimensional optical force clamp for single molecule studies, Biophys. J. 83 (2002) 491–501.
[21] A. Rohrbach, E.H. Stelzer, Three-dimensional position detection of optically trapped dielectric particles, J. Appl. Phys. 91 (2002) 5474–5488.
[22] J.F. Marko, E.D. Siggia, Stretching DNA, Macromolecules 28 (1995) 8759–8770.
[23] L.S. Lerman, Structural considerations in the interaction of deoxyribonucleic acid and acridines, J. Mol. Biol. 3 (1961) 18–30.
[24] F. Sanger, A.R. Coulson, G.F. Hong, D.F. Hill, G.B. Petersen, Nucleotide sequence of bacteriophage lambda DNA, J. Mol. Biol. 162 (4) (1982) 729–733.
[25] A.L. Lehninger, Bioenergetics, W.A. Benjamin Press, Menlo Park, 1965.